THE JOURNAL OF PHYSICAL CHEMISTRY C

Article

Cite This: J. Phys. Chem. C 2019, 123, 10974−10980

pubs.acs.org/JPCC

Adsorption of Phosphonic-Acid-Functionalized Porphyrin Molecules on TiO_2(110)

Cynthia C. Fernández,[†] Daniel Wechsler,[‡] Tulio C. R. Rocha,[§] Hans-Peter Steinrück,[‡] Ole Lytken,*[,‡] and Federico J. Williams*[,†,‡]

[†]Departamento de Química Inorgá;nica, Analítica y Química Física, Facultad de Ciencias Exactas y Naturales, INQUIMAE-CONICET, Universidad de Buenos Aires, Ciudad Universitaria, Pabellón 2, Buenos Aires C1428EHA, Argentina

[‡]Lehrstuhl für Physikalische Chemie II, Universität Erlangen-Nürnberg, Egerlandstraße 3, Erlangen 91058, Germany

[§]Brazilian Synchrotron Light Laboratory (LNLS), Brazilian Center for Research on Energy and Materials (CNPEM), Campinas 13083-970, Brazil

ABSTRACT: We studied the adsorption geometry and bonding of mono- and tetraphosphonic-acid-functionalized tetraphenylporphyrin molecules on rutile TiO_2(110) surfaces. The investigation was carried out by means of X-ray photoelectron spectroscopy and near edge X-ray absorption fine structure (NEXAFS) measurements. We found that the molecules bind covalently to the surface in a mixed monodentate and bidentate mode implying deprotonation of one or two phosphonate hydroxyl groups. Our NEXAFS data suggest that molecules containing one functional phosphonic acid group are on average tilted further away from the surface than molecules with four functional groups. The highest occupied electronic state of both molecules is in the band gap at 2.1 eV below the Fermi level. Our results demonstrate that the number of functional phosphonic acid groups determine the adsorption geometry of tetraphenylporphyrins.

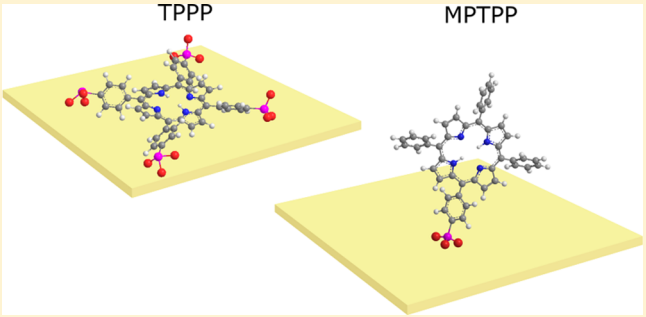

INTRODUCTION

Production of energy from renewable sources, driven by the growing energy demand and global warming, is at the forefront of current scientific research. As solar energy is the most abundant renewable energy source, a number of photovoltaic technologies have been developed to generate electric power after the absorption of photons. Presently, the dominant photovoltaic cells employed are based on silicon.[1] However, there are alternative developments with comparable or higher efficiencies based on dye-sensitized solar cells (DSSCs)[2] and perovskite solar cells.[3] DSSC-based photovoltaic devices have been studied extensively,[4] because they offer a flexible technology with a reasonable sunlight to electric power conversion efficiency and low-cost production.[5]

DSSCs are based on light-harvesting sensitizer molecules adsorbed on wide-band-gap semiconductors such as TiO_2. Porphyrin molecules are efficient sensitizers for DSSCs due to the strong absorption in the visible region, good photostability, and facile tuning of their electronic structure.[6] The molecules can be attached to the TiO_2 surface using different anchoring groups. The most commonly employed groups are carboxylic acids; however, phosphonic acids are also used as an alternative,[7] in particular, because of their strong bond to the surface. The anchoring mode and adsorption geometry of the molecules could limit charge transfer and charge recombination at the molecule/semiconductor interface and thus the overall light-to-electron conversion efficiency.[8−11] Therefore, a fundamental understanding of the molecular and electronic structure of porphyrins adsorbed on TiO_2 surfaces is required.

The interaction of porphyrin molecules with metal and well-defined oxide surfaces has been studied extensively.[12−15] Furthermore, there are recent fundamental studies on the adsorption of carboxylic-acid-functionalized porphyrins on TiO_2 single-crystal surfaces but none on the adsorption of phosphonic-acid-functionalized molecules. These studies show that the adsorption geometry depends on the number and position of the anchoring groups, and in some cases on the molecular coverage.[16−21] Porphyrins with one carboxylic acid functional group bind covalently to TiO_2(110) rutile surfaces after the carboxylic acid group has deprotonated. Raising the temperature to 600 K results in decomposition of the anchoring group while the macrocycle remains intact on the surface.[16] At low coverages, molecules with one carboxylic acid functional group are flat-lying on TiO_2(110)-2 × 1, whereas at monolayer coverage they are upright standing.[17] A similar behavior is observed when Zn protoporphyrins are adsorbed on TiO_2(110) surfaces.[18] The molecules bind covalently after deprotonation of the carboxylic acid functional groups at room

Received: January 31, 2019
Revised: March 24, 2019
Published: April 9, 2019

DOI: 10.1021/acs.jpcc.9b01019
J. Phys. Chem. C 2019, 123, 10974−10980

temperature. Also, at low coverages they adsorb with the macrocycle largely parallel to the substrate, whereas at monolayer coverage they reorient to an upright standing adsorption geometry. Zn tetraphenyl porphyrins with two carboxylic acid functional groups in a trans configuration adsorb with the macrocycle parallel to the surface. In this case, covalent bonds between the molecule and the surface are formed only after annealing.[19] Cu tetraphenyl porphyrins with four carboxylic acid functional groups adsorb with the macrocycle parallel to the TiO_2(110) substrate in two configurations that differ in the orientation with respect to the bridging oxygen rows.[20,21]

In this work, we investigated the bonding modes and the adsorption geometry of porphyrins functionalized with one or four phosphonic acid anchoring groups on rutile TiO_2(110). Specifically, we studied the adsorption of 5-mono(4-phosphonophenyl)-10,15,20-triphenyl porphyrin (MPTPP) and meso-tetra(4-phosphonophenyl) porphyrin (TPPP) molecules (Figure 1). We used synchrotron radiation X-ray photoelectron spectroscopy (XPS) to determine the bonding modes and the occupied molecular electronic states. We also employed near edge X-ray absorption fine structure (NEXAFS) measurements to determine the molecular orientation. Our results highlight the importance of the number of functional groups on the molecular orientation of adsorbed porphyrin molecules.

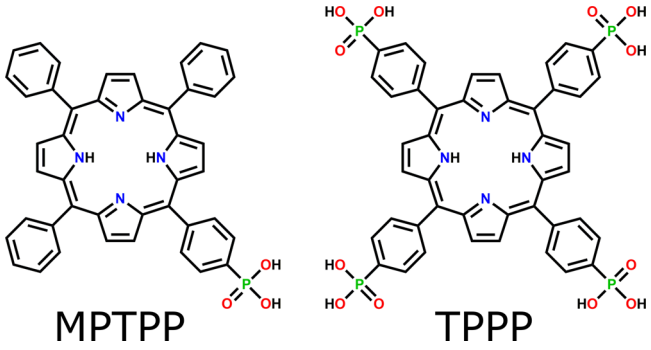

Figure 1. Molecular structure of the mono- and tetraphosphonic-acid-functionalized porphyrin molecules. MPTPP: 5-mono(4-phosphonophenyl)-10,15,20-triphenyl porphyrin and TPPP: meso-tetra(4-phosphonophenyl) porphyrin.

EXPERIMENTAL METHODS

The synchrotron-based XPS and total-electron-yield NEXAFS measurements were carried out at the Brazilian Synchrotron Light Source (LNLS), Campinas, Brazil, using the Photoemission End Station of the planar grating monochromator (PGM) beamline with a base pressure of 2×10^{-10} mbar. All spectra were normalized to the photon flux measured using a gold mesh. The rutile TiO_2(110) single crystals were cleaned in vacuum by sputtering and annealing. The clean crystals were then transferred into air and immediately brought into contact with 0.1 mM MPTPP or TPPP solutions in ethanol for 1 min. After removal from the solutions, the samples were rinsed rigorously in a stream of 25 mL ethanol from a syringe. To minimize the nonvolatile residue deposited on the TiO_2(110) crystal as the ethanol used for rinsing evaporates, as much ethanol as possible was blown off the sample using an argon jet before the remaining thin film of ethanol was allowed to evaporate from the sample. Thereafter, the samples were immediately transferred back into UHV. Here, we note that exposure of TiO_2(110) surfaces to air should result in the adsorption of carboxylic acids present in air in parts per billion.[22] However, we expect these adsorbates to be replaced by porphyrin molecules in solution. Porphyrin coverages are based on the N 1s to Ti 2p ratios, using a free base 5,10,15,20-tetraphenyl porphyrin (2HTPP) monolayer, obtained by multilayer desorption, as reference. Thus, one monolayer corresponds to the amount of nitrogen equivalent to a flat-lying layer of 2HTPP on TiO_2(110).[23]

RESULTS AND DISCUSSION

The N 1s, P 2p, and O 1s spectra obtained by synchrotron-based XPS after adsorption of 0.9 ML of MPTPP and 0.7 ML of TPPP on TiO_2(110) are shown in Figure 2. N 1s was measured with a photon energy of 500 eV, P 2p with 270 eV and O 1s with 650 eV. The N 1s spectra show the characteristic two peaks of metal-free porphyrins at 400.0 and 398.0 eV, due to the aminic (−NH−) and the iminic (=N−) nitrogen atoms in the macrocycle.[24] In principle, we

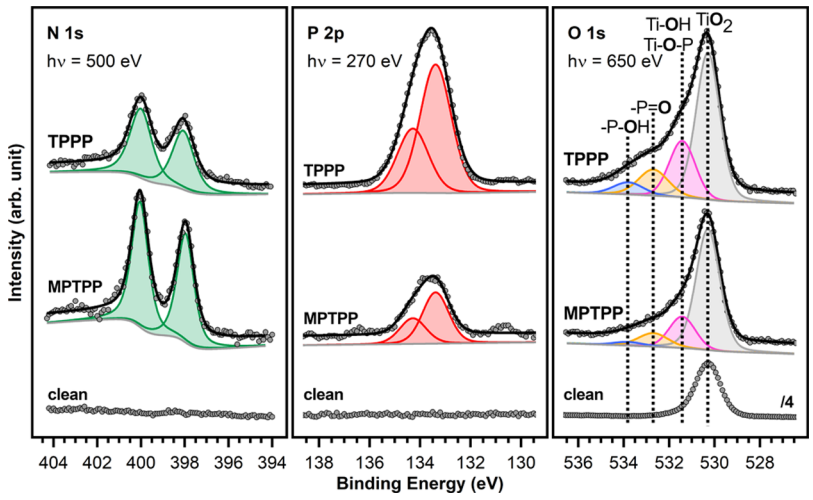

Figure 2. N 1s, P 2p, and O 1s synchrotron-based XPS spectra measured after the adsorption of 0.9 ML MPTPP and 0.7 ML TPPP on rutile TiO_2(110).

DOI: 10.1021/acs.jpcc.9b01019
J. Phys. Chem. C 2019, 123, 10974−10980

expect peaks of equal intensities. However, the aminic component is slightly larger. This has been previously assigned to protonated porphyrin diacid molecules, formed after the iminic nitrogen atoms capture protons from hydroxyl groups present on the surface.[23,25] Smaller effects, on the order of 10%, have also been observed in multilayers, due to the shake-up satellite of the iminic nitrogen atoms overlapping with the main peak of the aminic nitrogen atoms.[26]

The P 2p spectra show the expected spin-orbit-split doublet of a single species, with the P $2p_{3/2}$ component at 133.4 eV and the P $2p_{1/2}$ component at 134.3 eV, in agreement with phosphorous in phosphonic acid adsorbed on TiO_2.[27] Both O 1s spectra show a large signal at 530.3 eV, due to the substrate oxide peak, and a high-binding-energy shoulder, caused by the oxygen atoms of the phosphonate group. This shoulder can be fitted with three additional peaks of identical shape. These three peaks have previously been ascribed to P−OH and P═O of intact phosphonic acid at 533.9 and 532.7 eV, respectively,[28−30] in addition to linking oxygen atoms (P−O−Ti) and surface hydroxyl groups (Ti−OH) overlapping at 531.4 eV.[27,31] This later contribution can be seen after exposure of TiO_2(110) to water vapour.[32] Figure 3 illustrates

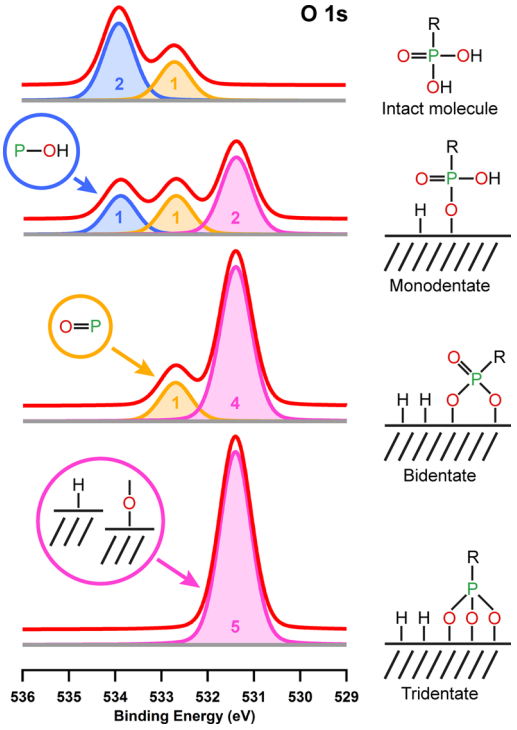

Figure 3. Bonding modes of phosphonic-acid-functionalized molecules on oxide surface together with their expected schematically sketched O 1s XPS spectra.

schematically how the ratios between these three components are expected to change depending on the binding motif of the phosphonic acid linker group.[33−35] The ratios we observe, from high to low binding energies, are 0.4:1:2.2 for MPTPP and for TPPP, which is in agreement with a mixture of 40% monodentate and 60% bidentate and a loss of protons to the solution. This assignment is, however, only tentative, especially for the four-fold functionalized TPPP molecule. For TPPP, a non-flat-lying adsorption geometry would result in at least two of the phosphonic acid groups pointing away from the surface, which are therefore not involved in chemical bonding. Furthermore, these groups could be deprotonated (with a counter ion). In addition, the low attenuation length at the 100 eV kinetic energy of the O 1s photoelectrons would result in a larger damping of the signal from the groups forming the bond to the surface. All this combined makes the unambiguous determination of the binding mode by XPS not possible.

The binding mode of phosphonic acid functional groups on TiO_2 depends on the surface coverage and on the structure of the underlying substrate.[33,36−38] For instance, on anatase TiO_2(101) the tridentate mode does not form,[36] and thus phenyl and alkyl phosphonic acid adsorb at low coverage in a bidentate mode and at high coverage in a mixed monodentate and bidentate mode.[37,38] On anatase TiO_2(001), however, the bidentate and tridentate modes are both stable.[36] The situation is also different on rutile TiO_2(110), where methyl phosphonic acid is adsorbed in a bidentate mode at 0.5 ML.[35] The tridentate adsorption mode is typically assigned on the basis of the disappearance of the −P═O IR signal.[39] However, IR alone should not be used to determine the binding mode as adsorption on TiO_2 results in a considerable shift of the −P═O stretching frequency to a lower wave number overlapping with other signals. Thus, its disappearance cannot be used to assign a particular binding mode.[36] Indeed, density functional theory (DFT) calculations show that the tridentate mode is energetically unfavorable on both rutile TiO_2(110) and anatase TiO_2(101) because of the molecular strain induced by the distance between the Ti rows.[36,40,41] This suggests that the tridentate mode should not be present in our experiments, which supports our assignment of a mixture of 40% monodentate and 60% bidentate for the MPTPP layer. As discussed above, for TPPP the assignment is only valid if the molecule is flat-lying.

Figure 4 shows the N K-edge NEXAFS spectra for different photon incidence angles after deposition from solution of

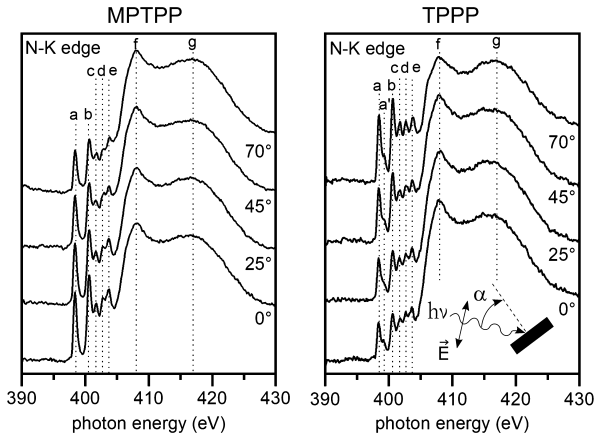

Figure 4. 0.9 ML MPTPP and 0.7 ML TPPP N K-edge NEXAFS spectra measured at different angles between the crystal surface normal and the photon propagation direction.

MPTPP (left panel) and TPPP (right panel) on TiO_2(110). All the spectra were recorded with the electric field vector aligned along the [001] direction. The photon incidence angle, α, was varied between 0° (normal incidence) and 70° (grazing incidence), varying the polar angle of the electric field vector with respect to the surface normal between 90° (normal incidence) and 20° (grazing incidence).

The N K-edge NEXAFS spectra show seven peaks labeled a−g. The peaks at 398.5 (a), 400.5 (b), 401.7 (c), 402.7 (d),

DOI: 10.1021/acs.jpcc.9b01019
J. Phys. Chem. C 2019, 123, 10974−10980

and 403.7 (e) eV are assigned to transitions from the iminic N 1s and the aminic N 1s to different π^* orbitals in the porphyrin ring.[42] Furthermore, the spectra contain two broad peaks at approximately 408 (f) and 417 (g) eV due to transitions to σ^* orbitals.[42] Finally, the spectra display a peak at 399.3 (a′) eV, which is not present in the free-base porphyrin without the functional groups, and we therefore suggest that it is due to π^* transitions in the protonated molecules present on the surface.

The intensity of the N 1s to π^* transitions depends on the orientation of the electric field vector of the polarized radiation relative to the transition dipole moment. Hence, information on the molecular orientation can be deduced from the angular dependence of the π^* peaks.[43] For aromatic rings, the N 1s to π^* transition is polarized perpendicular to the molecular plane, and thus maximum intensity is observed when the electric field vector is perpendicular to the molecular plane. The opposite is true for N 1s to σ^* transitions: maximum intensity is observed when the electric field vector is parallel to the molecular plane. Figure 4 shows that for MPTPP the π^* intensity increases and the σ^* intensity decreases as the photon incidence angle decreases, suggesting an upright standing macrocycle. The opposite behavior is observed for TPPP, where the π^* intensity decreases and the σ^* intensity increases as the photon incidence angle decreases, which suggests an adsorption geometry with the macrocycle closer to the surface.

Figure 5 shows the quantitative analysis of the angular dependence of the π^* resonance at 398.5 eV, for MPTPP (red)

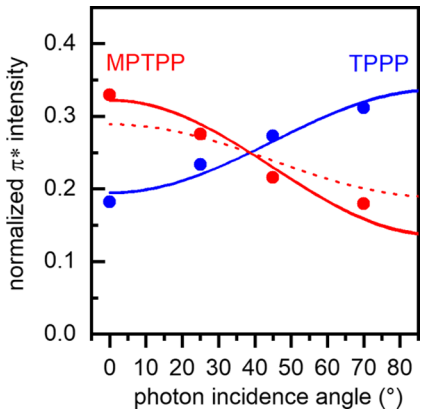

Figure 5. Angular dependence of the π^* transitions of the nitrogen K-edge of MPTPP and TPPP on TiO_2(110). The solid lines represent the fits for the range of azimuthal orientations producing a good fit to the data. This yields upper and lower limits on the polar angles of the molecules of 75° ± 15° for MPTPP and 50° ± 15° for TPPP. The dashed red line corresponds to an azimuthal angle of 70° and a polar angle of 90°.

and TPPP (blue) adsorbed on TiO_2(110), based on the spectra in Figure 4. Ideally, for two-fold symmetry substrates such as TiO_2(110), angle-resolved NEXAFS should be recorded using at least two different azimuthal incidence angles. However, the data in Figure 4 were acquired at only one azimuthal incidence angle. This imposes some limitations concerning the unequivocal determination of the polar and azimuthal orientation of the molecule. Nevertheless, it is possible to determine upper and lower limits on the polar angles of the molecules, by fitting the data for all possible azimuthal orientations and extracting only those producing an acceptable fit to the measured data. If the molecules are not aligned along the surface normal and the high-symmetry direction of the substrate, then one gets four domains which were used to fit the data. The angular dependence of MPTPP can only be fitted for azimuthal angles between 0° and 60°, yielding polar angles ranging from 60° to 90°. Increasing the azimuthal angle beyond 60° results in a significantly worse fit to the measured data, as illustrated by the dashed red line in Figure 5 corresponding to an azimuthal angle of 70° and a polar angle of 90°. TPPP can be fitted for any azimuthal angle, resulting in polar angles between 35° and 65°. This means that, despite having only measured at one azimuthal angle, we are still able to give a range of possible polar angles for the two molecules: 75° ± 15° for MPTPP and 50° ± 15° for TPPP. The angle of 75° deduced for MPTPP is in good agreement with the reported angles (65−80°) for phenyl phosphonic acid on indium oxide,[44] zinc oxide,[45] and anatase TiO_2(101) surfaces.[37] This suggests that MPTPP could grow in islands of upright-standing molecules at a coverage of 0.9 ML, where the surface could still accommodate all molecules in a flat-lying geometry. For TPPP, the range of possible angles include 35°, which is the angle observed for flat-lying tetraphenyl porphyrin molecules because of their saddle-shape distortion, with two opposing pyrrole rings pointing upward and the other two down toward the surface.[46] The distorted structure deduced from DFT can be found elsewhere.[47] It is thus entirely possible that TPPP at 0.7 ML adsorbs in a flat-lying configuration with all four phosphonic acid groups bonded to the surface. Such a flat-lying configuration would also explain the absence of intact phosphonic acid groups in the O 1s spectrum. Notably, the valence band spectra discussed below also suggest that the TPPP macrocycle could be interacting with the surface, in line with a flat-lying adsorption geometry.

Figure 6 shows the P $L_{2,3}$ edge NEXAFS spectra of MPTPP and TPPP on TiO_2(110). The spectra show peaks at 133.5 (a),

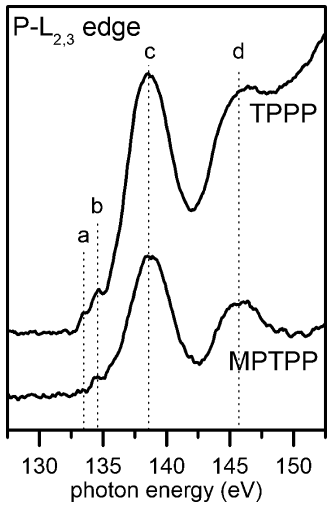

Figure 6. P $L_{2,3}$ edge NEXAFS spectra of 0.9 ML MPTPP and 0.7 ML TPPP adsorbed on TiO_2(110).

134.5 (b), 138.5 (c), and 148.5 (d) eV. The peaks at 133.5 and 134.5 eV are due to transitions from $2p_{3/2}$ and $2p_{1/2}$ into the first unoccupied antibonding state with 3s character. The peak at 138.5 eV corresponds to a transition into an antibonding state with mixed character, and the peak at 145.8 eV to a transition into an antibonding state with 3d character.[48] These peaks are observed for a broad range of inorganic and organic phosphorous containing compounds, and their relative

DOI: 10.1021/acs.jpcc.9b01019
J. Phys. Chem. C 2019, 123, 10974−10980

positions and intensities depend on the local electronic environment of the P atom.[48,49] Therefore, the P $L_{2,3}$ edge NEXAFS spectra can be used for the speciation of P-containing organic compounds. Notably, the spectra in Figure 6 differ from the reference spectrum of phenyl phosphonic acid as this latter one has extra peaks at 136.5 and 137.4 eV.[48] This indicates that the electronic environment in the P atom changes when the molecule binds to the surface, which is in line with the phosphonic acid deprotonation and with the formation of new −Ti−O−P− bonds as suggested by XPS.

It is also important to determine whether the number of phosphonic acid functional groups causes a change in the electronic structure of the adsorbed molecules. Figure 7 shows

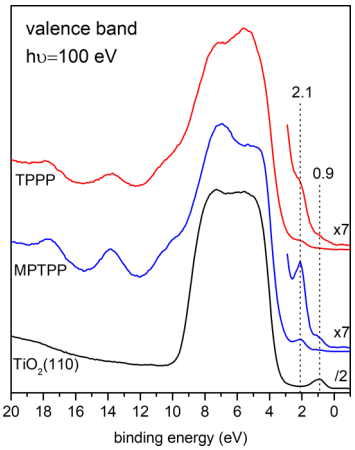

Figure 7. Valence-band photoemission spectra corresponding to the clean TiO_2(110) rutile surface (bottom) and to MPTPP (blue) and TPPP (red) adsorbed on TiO_2(110).

the valence band spectra measured at the synchrotron using a photon energy of 100 eV. The bottom spectrum corresponding to the clean TiO_2(110) rutile surface shows a broad O 2p band from 3.4 to 10 eV, in excellent agreement with previous reports.[50] Furthermore, the spectrum also shows a band-gap state about 0.9 eV below the Fermi level, which has been assigned to a Ti^{3+} defect state due to the presence of oxygen vacancies.[51] The blue and red spectra correspond to MPTPP and TPPP adsorbed on TiO_2(110), respectively. The spectra show four clearly resolved peaks at 2.1, 10.5, 13.7, and 17.6 eV, due to photoemission from different molecular orbitals. Furthermore, the change in the shape of the O 2p bands observed in both spectra suggests that there are other molecular electronic states overlapping with the substrate band. The highest occupied molecular orbital (HOMO) is located in the band gap at 2.1 eV below the Fermi level and corresponds to an electronic state with high electronic density at the macrocycle.[52] Notably, we also observe this state after adsorption of the same molecule replacing the phosphonic acid group with a carboxylic acid group. Finally, the Ti^{3+} defect state of the substrate at 0.9 eV is attenuated, but still present after adsorption of the molecules.

Finally, we should note that for MPTPP the HOMO peak (blue spectrum in Figure 7) is a very well-defined sharp peak, whereas for TPPP is a broader peak. Tentatively, one could attribute the broadening to an interaction of the HOMO with the substrate. Given that this electronic state has the largest electronic density at the macrocycle, the different shapes observed in the valence band are in line with upright standing MPTPP molecules and flat-lying TPPP molecules as suggested by the NEXAFS data discussed above.

CONCLUSIONS

Phosphonic-acid-functionalized tetraphenyl-porphyrin molecules adsorb from solution on rutile TiO_2(110) single-crystal surfaces in a mixed monodentate and bidentate bonding configuration. Molecules with one phosphonic acid functional group adsorb with the macrocycle tilted 75° ± 15° with respect to the surface, consistent with a mostly upright-standing bidentate anchoring mode. Increasing the number of phosphonic acid groups to four results in a decrease in the macrocycle tilt angle to 50° ± 15°. Notably, the uncertainty arising from our limited data set includes an angle of 35°, which would be in line with a flat-lying macrocycle, exhibiting the saddle-shape deformation observed for flat-lying tetraphenyl porphyrin molecules. The HOMOs of MPTPP and TPPP are located in the band gap at 2.1 eV below the Fermi level, and the broadening observed in the TPPP HOMO is compatible with a macrocycle interacting with the substrate. Our results highlight the importance of the number of anchoring groups on the properties of adsorbed porphyrin molecules and are relevant in the design of molecular devices based on porphyrins adsorbed on oxide surfaces.

AUTHOR INFORMATION

Corresponding Authors

*E-mail: ole.lytken@fau.de (O.L.).
*E-mail: fwilliams@qi.fcen.uba.ar (F.J.W.).

ORCID

Hans-Peter Steinrück: 0000-0003-1347-8962
Ole Lytken: 0000-0003-0572-0827
Federico J. Williams: 0000-0002-6194-2734

Notes

The authors declare no competing financial interest.

ACKNOWLEDGMENTS

This project was financially supported by the Deutsche Forschungsgemeinschaft (DFG) within the Research Unit FOR 1878 funCOS—Functional Molecular Structures on Complex Oxide Surfaces. C.C.F. and F.J.W. acknowledge support from the Consejo Nacional de Investigaciones Científicas y Técnicas (CONICET). F.J.W. thanks DFG for financial funding through a Mercator Fellowship. F.J.W. acknowledges financial support from the Brazilian Synchrotron Light Laboratory (LNLS) for the use of the PGM-U11 beamline.

REFERENCES

(1) Battaglia, C.; Cuevas, A.; De Wolf, S. High-Efficiency Crystalline Silicon Solar Cells: Status and Perspectives. *Energy Environ. Sci.* **2016**, *9*, 1552−1576.
(2) O'Regan, B.; Grätzel, M. A Low-Cost, High-Efficiency Solar Cell Based on Dye-Sensitized Colloidal TiO2 Films. *Nature* **1991**, *353*, 737−740.
(3) Zhang, W.; Eperon, G. E.; Snaith, H. J. Metal Halide Perovskites for Energy Applications. *Nat. Energy* **2016**, *1*, 16048.
(4) Hagfeldt, A.; Boschloo, G.; Sun, L.; Kloo, L.; Pettersson, H. Dye-Sensitized Solar Cells. *Chem. Rev.* **2010**, *110*, 6595−6663.
(5) Fakharuddin, A.; Jose, R.; Brown, T. M.; Fabregat-Santiago, F.; Bisquert, J. A Perspective on the Production of Dye-Sensitized Solar Modules. *Energy Environ. Sci.* **2014**, *7*, 3952−3981.

DOI: 10.1021/acs.jpcc.9b01019
J. Phys. Chem. C 2019, 123, 10974−10980

(6) Higashino, T.; Imahori, H. Porphyrins as Excellent Dyes for Dye-Sensitized Solar Cells: Recent Developments and Insights. *Dalt. Trans.* **2015**, *44*, 448−463.
(7) Abate, A.; Pérez-Tejada, R.; Wojciechowski, K.; Foster, J. M.; Sadhanala, A.; Steiner, U.; Snaith, H. J.; Franco, S.; Orduna, J. Phosphonic Anchoring Groups in Organic Dyes for Solid-State Solar Cells. *Phys. Chem. Chem. Phys.* **2015**, *17*, 18780−18789.
(8) Clifford, J. N.; Yahioglu, G.; Milgrom, L. R.; Durrant, J. R. Molecular Control of Recombination Dynamics in Dye Sensitised Nanocrystalline TiO_2 Films. *Chem. Commun.* **2002**, *12*, 1260−1261.
(9) Clifford, J. N.; Palomares, E.; Nazeeruddin, M. K.; Grätzel, M.; Nelson, J.; Li, X.; Long, N. J.; Durrant, J. R. Molecular Control of Recombination Dynamics in Dye-Sensitized Nanocrystalline TiO_2 Films: Free Energy vs Distance Dependence. *J. Am. Chem. Soc.* **2004**, *126*, 5225−5233.
(10) Ladomenou, K.; Kitsopoulos, T. N.; Sharma, G. D.; Coutsolelos, A. G. The Importance of Various Anchoring Groups Attached on Porphyrins as Potential Dyes for DSSC Applications. *RSC Adv.* **2014**, *4*, 21379−21404.
(11) Hart, A. S.; KC, C. B.; Gobeze, H. B.; Sequeira, L. R.; D'Souza, F. Porphyrin-Sensitized Solar Cells: Effect of Carboxyl Anchor Group Orientation on the Cell Performance. *ACS Appl. Mater. Interfaces* **2013**, *5*, 5314−5323.
(12) Auwärter, W.; Écija, D.; Klappenberger, F.; Barth, J. V. Porphyrins at Interfaces. *Nat. Chem.* **2015**, *7*, 105−120.
(13) Gottfried, J. M. Surface Chemistry of Porphyrins and Phthalocyanines. *Surf. Sci. Rep.* **2015**, *70*, 259−379.
(14) Diller, K.; Papageorgiou, A. C.; Klappenberger, F.; Allegretti, F.; Barth, J. V.; Auwärter, W. Vacuo Interfacial Tetrapyrrole Metallation. *Chem. Soc. Rev.* **2016**, *45*, 1629−1656.
(15) Marbach, H. Surface-Mediated in Situ Metalation of Porphyrins at the Solid−Vacuum Interface. *Acc. Chem. Res.* **2015**, *48*, 2649−2658.
(16) Wechsler, D.; Fernández, C. C.; Steinrück, H.-P.; Lytken, O.; Williams, F. J. Covalent Anchoring and Interfacial Reactions of Adsorbed Porphyrins on Rutile TiO_2(110). *J. Phys. Chem. C* **2018**, *122*, 4480−4487.
(17) Olszowski, P.; Zając, Ł.; Godlewski, S.; Such, B.; Jöhr, R.; Glatzel, T.; Meyer, E.; Szymonski, M. Role of a Carboxyl Group in the Adsorption of Zn Porphyrins on TiO_2 (011)-2×1 Surface. *J. Phys. Chem. C* **2015**, *119*, 21561−21566.
(18) Rienzo, A.; Mayor, L. C.; Magnano, G.; Satterley, C. J.; Ataman, E.; Schnadt, J.; Schulte, K.; O'Shea, J. N. X-Ray Absorption and Photoemission Spectroscopy of Zinc Protoporphyrin Adsorbed on Rutile TiO_2(110) Prepared by in Situ Electrospray Deposition. *J. Chem. Phys.* **2010**, *132*, 084703.
(19) Jöhr, R.; Hinaut, A.; Pawlak, R.; Zajac, Ł.; Olszowski, P.; Such, B.; Glatzel, T.; Zhang, J.; Muntwiler, M.; Bergkamp, J. J.; et al. Thermally Induced Anchoring of a Zinc-Carboxyphenylporphyrin on Rutile TiO_2(110). *J. Chem. Phys.* **2017**, *146*, 184704.
(20) Jöhr, R.; Hinaut, A.; Pawlak, R.; Sadeghi, A.; Saha, S.; Goedecker, S.; Such, B.; Szymonski, M.; Meyer, E.; Glatzel, T. Characterization of Individual Molecular Adsorption Geometries by Atomic Force Microscopy: Cu-TCPP on Rutile TiO_2(110). *J. Chem. Phys.* **2015**, *143*, 094202.
(21) Pawlak, R.; Sadeghi, A.; Jöhr, R.; Hinaut, A.; Meier, T.; Kawai, S.; Zajac, Ł.; Olszowski, P.; Godlewski, S.; Such, B.; et al. Hydroxyl-Induced Partial Charge States of Single Porphyrins on Titania Rutile. *J. Phys. Chem. C* **2017**, *121*, 3607−3614.
(22) Balajka, J.; Hines, M. A.; DeBenedetti, W. J. I.; Komora, M.; Pavelec, J.; Schmid, M.; Diebold, U. High-Affinity Adsorption Leads to Molecularly Ordered Interfaces on TiO_2 in Air and Solution. *Science* **2018**, *361*, 786−789.
(23) Köbl, J.; Wang, T.; Wang, C.; Drost, M.; Tu, F.; Xu, Q.; Ju, H.; Wechsler, D.; Franke, M.; Pan, H.; et al. Hungry Porphyrins: Protonation and Self-Metalation of Tetraphenylporphyrin on TiO_2(110)-1×1. *ChemistrySelect* **2016**, *1*, 6103−6105.
(24) Gassman, P. G.; Ghosh, A.; Almlof, J. Electronic Effects of Peripheral Substituents in Porphyrins: X-Ray Photoelectron Spectroscopy and Ab Initio Self-Consistent Field Calculations. *J. Am. Chem. Soc.* **1992**, *114*, 9990−10000.
(25) Lovat, G.; Forrer, D.; Abadia, M.; Dominguez, M.; Casarin, M.; Rogero, C.; Vittadini, A.; Floreano, L. Hydrogen Capture by Porphyrins at the TiO_2(110) Surface. *Phys. Chem. Chem. Phys.* **2015**, *17*, 30119−30124.
(26) Röckert, M.; Ditze, S.; Stark, M.; Xiao, J.; Steinrück, H.-P.; Marbach, H.; Lytken, O. Abrupt Coverage-Induced Enhancement of the Self-Metalation of Tetraphenylporphyrin with Cu(111). *J. Phys. Chem. C* **2014**, *118*, 1661−1667.
(27) Viornery, C.; Chevolot, Y.; Léonard, D.; Aronsson, B.-O.; Péchy, P.; Mathieu, H. J.; Descouts, P.; Grätzel, M. Surface Modification of Titanium with Phosphonic Acid To Improve Bone Bonding: Characterization by XPS and ToF-SIMS. *Langmuir* **2002**, *18*, 2582−2589.
(28) Tsud, N.; Yoshitake, M. Vacuum Vapour Deposition of Phenylphosphonic Acid on Amorphous Alumina. *Surf. Sci.* **2007**, *601*, 3060−3066.
(29) Textor, M.; Ruiz, L.; Hofer, R.; Rossi, A.; Feldman, K.; Hähner, G.; Spencer, N. D. Structural Chemistry of Self-Assembled Monolayers of Octadecylphosphoric Acid on Tantalum Oxide Surfaces. *Langmuir* **2000**, *16*, 3257−3271.
(30) Adden, N.; Gamble, L. J.; Castner, D. G.; Hoffmann, A.; Gross, G.; Menzel, H. Phosphonic Acid Monolayers for Binding of Bioactive Molecules to Titanium Surfaces. *Langmuir* **2006**, *22*, 8197−8204.
(31) Mani, G.; Johnson, D. M.; Marton, D.; Dougherty, V. L.; Feldman, M. D.; Patel, D.; Ayon, A. A.; Agrawal, C. M. Stability of Self-Assembled Monolayers on Titanium and Gold. *Langmuir* **2008**, *24*, 6774−6784.
(32) Wang, L.-Q.; Baer, D. R.; Engelhard, M. H.; Shultz, A. N. The Adsorption of Liquid and Vapor Water on TiO_2(110) Surfaces: The Role of Defects. *Surf. Sci.* **1995**, *344*, 237−250.
(33) Chen, Y.; Trzop, E.; Sokolow, J. D.; Coppens, P. Direct Observation of the Binding Mode of the Phosphonate Anchor to Nanosized Polyoxotitanate Clusters. *Chem.—Eur. J.* **2013**, *19*, 16651−16655.
(34) Bae, E.; Choi, W.; Park, J.; Shin, H. S.; Kim, S. B.; Lee, J. S. Effects of Surface Anchoring Groups (Carboxylate vs Phosphonate) in Ruthenium-Complex-Sensitized TiO_2 on Visible Light Reactivity in Aqueous Suspensions. *J. Phys. Chem. B* **2004**, *108*, 14093−14101.
(35) Pang, C. L.; Watkins, M.; Cabailh, G.; Ferrero, S.; Ngo, L. T.; Chen, Q.; Humphrey, D. S.; Shluger, A. L.; Thornton, G. Bonding of Methyl Phosphonate to TiO_2(110). *J. Phys. Chem. C* **2010**, *114*, 16983−16988.
(36) Geldof, D.; Tassi, M.; Carleer, R.; Adriaensens, P.; Roevens, A.; Meynen, V.; Blockhuys, F. Binding Modes of Phosphonic Acid Derivatives Adsorbed on TiO_2 Surfaces: Assignments of Experimental IR and NMR Spectra Based on DFT/PBC Calculations. *Surf. Sci.* **2017**, *655*, 31−38.
(37) Wagstaffe, M.; Thomas, A. G.; Jackman, M. J.; Torres-Molina, M.; Syres, K. L.; Handrup, K. An Experimental Investigation of the Adsorption of a Phosphonic Acid on the Anatase TiO_2(101) Surface. *J. Phys. Chem. C* **2016**, *120*, 1693−1700.
(38) Di Valentin, C.; Costa, D. Anatase TiO_2 Surface Functionalization by Alkylphosphonic Acid: A DFT+D Study. *J. Phys. Chem. C* **2012**, *116*, 2819−2828.
(39) Guerrero, G.; Mutin, P. H.; Vioux, A. Anchoring of Phosphonate and Phosphinate Coupling Molecules on Titania Particles. *Chem. Mater.* **2001**, *13*, 4367−4373.
(40) Luschtinetz, R.; Frenzel, J.; Milek, T.; Seifert, G. Adsorption of Phosphonic Acid at the TiO_2 Anatase (101) and Rutile (110) Surfaces. *J. Phys. Chem. C* **2009**, *113*, 5730−5740.
(41) Nilsing, M.; Lunell, S.; Persson, P.; Ojamäe, L. Phosphonic Acid Adsorption at the TiO_2 Anatase (101) Surface Investigated by Periodic Hybrid HF-DFT Computations. *Surf. Sci.* **2005**, *582*, 49−60.
(42) Polzonetti, G.; Carravetta, V.; Iucci, G.; Ferri, A.; Paolucci, G.; Goldoni, A.; Parent, P.; Laffon, C.; Russo, M. V. Electronic Structure of Platinum Complex/Zn-Porphyrinato Assembled Macrosystems, Related Precursors and Model Molecules, as Probed by X-Ray

DOI: 10.1021/acs.jpcc.9b01019
J. Phys. Chem. C 2019, 123, 10974−10980

Absorption Spectroscopy (NEXAFS): Theory and Experiment. *Chem. Phys.* **2004**, *296*, 87−100.
(43) Stöhr, J.; Outka, D. A. Determination of Molecular Orientations on Surfaces from the Angular Dependence of Near-Edge x-Ray-Absorption Fine-Structure Spectra. *Phys. Rev. B: Condens. Matter Mater. Phys.* **1987**, *36*, 7891−7905.
(44) Gliboff, M.; Sang, L.; Knesting, K. M.; Schalnat, M. C.; Mudalige, A.; Ratcliff, E. L.; Li, H.; Sigdel, A. K.; Giordano, A. J.; Berry, J. J.; et al. Orientation of Phenylphosphonic Acid Self-Assembled Monolayers on a Transparent Conductive Oxide: A Combined NEXAFS, PM-IRRAS, and DFT Study. *Langmuir* **2013**, *29*, 2166−2174.
(45) Ostapenko, A.; Klöffel, T.; Meyer, B.; Witte, G. Formation and Stability of Phenylphosphonic Acid Monolayers on ZnO: Comparison of In Situ and Ex Situ SAM Preparation. *Langmuir* **2016**, *32*, 5029−5037.
(46) Wechsler, D.; Franke, M.; Tariq, Q.; Zhang, L.; Lee, T.-L.; Thakur, P. K.; Tsud, N.; Bercha, S.; Prince, K. C.; Steinrück, H.-P.; et al. Adsorption Structure of Cobalt Tetraphenylporphyrin on Ag(100). *J. Phys. Chem. C* **2017**, *121*, 5667−5674.
(47) Lepper, M.; Köbl, J.; Schmitt, T.; Gurrath, M.; de Siervo, A.; Schneider, M. A.; Steinrück, H.-P.; Meyer, B.; Marbach, H.; Hieringer, W. "Inverted" Porphyrins: A Distorted Adsorption Geometry of Free-Base Porphyrins on Cu(111). *Chem. Commun.* **2017**, *53*, 8207−8210.
(48) Kruse, J.; Leinweber, P.; Eckhardt, K.-U.; Godlinski, F.; Hu, Y.; Zuin, L. Phosphorus L 2,3 -Edge XANES: Overview of Reference Compounds. *J. Synchrotron Radiat.* **2009**, *16*, 247−259.
(49) Yin, Z.; Kasrai, M.; Fuller, M.; Bancroft, G. M.; Fyfe, K.; Tan, K. H. Application of Soft X-Ray Absorption Spectroscopy in Chemical Characterization of Antiwear Films Generated by ZDDP Part I: The Effects of Physical Parameters. *Wear* **1997**, *202*, 172−191.
(50) Rangan, S.; Katalinic, S.; Thorpe, R.; Bartynski, R. A.; Rochford, J.; Galoppini, E. Energy Level Alignment of a Zinc(II) Tetraphenylporphyrin Dye Adsorbed onto TiO_2 (110) and ZnO($11\bar{2}0$) Surfaces. *J. Phys. Chem. C* **2010**, *114*, 1139−1147.
(51) Yim, C. M.; Pang, C. L.; Thornton, G. Oxygen Vacancy Origin of the Surface Band-Gap State of TiO_2(110). *Phys. Rev. Lett.* **2010**, *104*, 036806.
(52) Giovanelli, L.; Lee, H.-L.; Lacaze-Dufaure, C.; Koudia, M.; Clair, S.; Lin, Y.-P.; Ksari, Y.; Themlin, J.-M.; Abel, M.; Cafolla, A. A. Electronic Structure of Tetra(4-Aminophenyl)Porphyrin Studied by Photoemission, UV−Vis Spectroscopy and Density Functional Theory. *J. Electron. Spectrosc. Relat. Phenom.* **2017**, *218*, 40−45.

DOI: 10.1021/acs.jpcc.9b01019
J. Phys. Chem. C 2019, 123, 10974−10980